ELSEVIER

Journal of Photochemistry and Photobiology A: Chemistry 150 (2002) 261–269

Journal of Photochemistry and Photobiology A:Chemistry

www.elsevier.com/locate/jphotochem

Short communication

Comparison of the processes induced by nitrogen dilution on the photodissociation of silane and disilane at 193 nm

B. Aka [a,*], E. Boch [b]

[a] *Département des Sciences et Technologie, Ecole Normale Supérieure d'Abidjan, 22 BP, Abidjan 22, 1561 Ivory Coast*
[b] *Centre de Recherches Nucléaires—Laboratoire PHASE, 23, rue du Loess, F-67037 Strasbourg Cedex, France*

Received 12 October 2001; received in revised form 26 November 2001; accepted 6 December 2001

Abstract

We compare the influence of the dilution of silane and disilane in nitrogen during laser photodissociation to produce silicon at 193 nm, at room temperature in a static reaction chamber. The experimental results show that the conversion of the reactant gas and its deposition yield can be controlled by varying adequately the extent of dilution. So, two total pressure regions have been observed, independent of the dilution: below 40–50 Torr, the variations of stable species concentration are very important but above these values the variation in the dilution rate has practically no effects on their concentrations. In the first region, during the silane photodissociation at the initial reactant pressure below 5 Torr, the conversion of silane increases with increasing dilution, and at higher initial reactant pressure the conversion of silane tends to rise only a little. In contrast, at any initial reactant pressure, the conversion of disilane during its photodecomposition decreases with increasing dilution. In the second region, the concentration of each stable gaseous species tends to reach a pressure stationary-state. For both the silane and disilane photodissociation, the deposition yield of silicon increases with decreasing the initial reactant gas pressure and it reaches a pressure stationary-state above 50% dilution; but in all the cases, it is greater in disilane photolysis than that of silane. A simple kinetic model is proposed for which the computed results predict the time-evolution of gas composition and amount of silicon deposited.

Keywords: (Di)silane; ArF laser; Photo-CVD; Absorption; Dilution; Nitrogen; Thermalization

1. Introduction

Over the past few years, there has been an increasing interest in photo-assisted chemical vapour deposition (photo-CVD) techniques for the production of thin insulating films such as SiO_2, SiN, Si_3N_4 or amorphous semiconductors films such as a-Si:H, a-Ge:H, a-SiC:H, [1–7].

These materials are deposited from the photodissociation of the reactant gas generally SiH_4 or Si_2H_6 mixed with buffer gases such as a rare gas (Ar, He), hydrogen (H_2) or nitrogen (N_2) [6,8–13].

Dilution is required for both economical and safety reasons since the presence of an inert gas at high enough concentration eliminates the explosive character of some mixtures or reactions like silanes + O_2 or silanes + NO, and generally it modifies the conversion of the reactant gas [8–10,14–17]. N_2 is an inert gas which does not interfere as a reactant or product in the photodecomposition reaction scheme contrary to the buffer gas H_2 [12,18,19].

Many studies have been reported on the photodissociation of silane (SiH_4) and disilane (Si_2H_6) at various wavelengths [20–32]. At the wavelength of 193 nm ($h\nu = 6.4$ eV), SiH_4 molecules cannot be decomposed by a single-photon excitation process, because absorption of SiH_4 starts only below 160 nm (over 7.8 eV) unlike 200 nm (over 6.2 eV) for Si_2H_6. Ten years ago, we [20,22] measured a silane bi-photonic absorption cross-section of 6×10^{-44} cm^4 s and disilane single-photon cross-section of 2×10^{-18} cm^2 added by small bi-photonic absorption contribution with a cross-section of 7.8×10^{-43} cm^4 s.

Among the energetically feasible reactions, the main initiation reactions during the photolysis of SiH_4 and Si_2H_6 reactants are [20–27], first for SiH_4

$$SiH_4 + 2h\nu \rightarrow SiH_3 + H, \quad \Delta H = 376\,\text{kJ/mol}\,(3.9\,\text{eV/molecule}) \qquad (R_1)$$

* Corresponding author. Tel. +225-2244-4232; fax: +225-2244-4232.
E-mail address: akabm@ci.refer.org (B. Aka).

1010-6030/02/$ – see front matter
PII: S1010-6030(01)00660-8

$$SiH_4 + 2h\nu \rightarrow SiH_2 + 2H,$$
$$\Delta H = 865\,kJ/mol\ (7.1\,eV/molecule) \quad (R_2)$$

then for Si_2H_6

$$Si_2H_6 + 1\,and/or\,2h\nu \rightarrow Si_2H_5 + H,$$
$$\Delta H = 359\,kJ/mol\ (3.14\,eV/molecule) \quad (R_3)$$

$$Si_2H_6 + 1\,and/or\,2h\nu \rightarrow Si_2H_4 + 2H,$$
$$\Delta H = 594\,kJ/mol\ (5.20\,eV/molecule) \quad (R_4)$$

$$Si_2H_6 + 1\,and/or\,2h\nu \rightarrow SiH_3 + SiH_3,$$
$$\Delta H = 318\,kJ/mol\ (3.29\,eV/molecule) \quad (R_5)$$

$$Si_2H_6 + 1\,and/or\,2h\nu \rightarrow SiH_3 + SiH_2 + H,$$
$$\Delta H = 619\,kJ/mol\ (6.42\,eV/molecule) \quad (R_6)$$

with ΔH being the reaction enthalpy.

Now, relatively little is known about the influence of nitrogen dilution on ArF laser photo-assisted CVD at 193 nm. It was therefore of interest to study the gas phase composition of stable species and the deposition yield of silicon as a function of dilution in N_2 and compare the behaviour of mixtures SiH_4 or Si_2H_6 added to such buffer gas.

2. Experimental

Silane or disilane, sealed in a suprasil quartz cylindrical reaction chamber ($Ø = 3$ cm, $L = 10$ cm) at pressures ranging between 5 and 20 Torr, is diluted in N_2 in percentage ($[N_2]/([N_2] + [SiH_4])$ or $[N_2]/([N_2] + [Si_2H_6])$) varying from 0 to 90 before being irradiated under normal incidence with a Lambda Physik (EMG 201 MSC) ArF excimer laser providing a resonance line at 193 nm, pulses of 20 ns duration. The reactor is continuously moved around and along its axis in order to irradiate a clean and silicon free area, so that the incident intensity should remain constant (Fig. 1).

The volume of the irradiated channel ($0.25\,cm^2 \times 3$ cm) is small enough with regard to the reactor volume ($\sim 71\,cm^3$) to consider that the stable species like SiH_4 or Si_2H_6, created during the laser pulse diffuse out of the channel and do not re-cross the photon beam.

The final pressures of stable species (mainly SiH_4, Si_2H_6, H_2) have been determined after ($125\,mJ/cm^2$ pulse, 10 Hz) using a condensation technique previously described [21,25,28]. In our experiments, Si_3H_8 or higher silanes did not appear at sufficiently high pressures to be revealed by the condensation technique, the precision of which has been estimated to be in the order of 10%. This should not be surprising because Si_3H_8 often represents less than 5% of gas phase composition [13,16,28,30]. All the reactions involving heavier silanes are therefore neglected in this study.

For all the following experiments, we have measured the final composition of the gas phase by varying both initial pressure of (di)silane and nitrogen dilution rate, after 1800 irradiation pulses (or 3 min) for silane source gas and 600 irradiation pulses for disilane source gas because in this latter case a red-brown deposit along the reactor appears more quickly and attenuates the incident light intensity.

3. Results and discussion

3.1. Effect of nitrogen dilution on gas composition

After the UV excitation of the reactant gas (SiH_4 or Si_2H_6), the gas phase is composed mainly of radical species (H, SiH_2, SiH_3, Si_2H_4, Si_2H_5), stable gaseous species (H_2, SiH_4, Si_2H_6), and there is a solid phase of silicon in amorphous, clusters or powder form. The fraction of silicon atoms (Si) which are in a solid form is calculated by material-balance from the measured pressures of stable gaseous species.

Material-balance during the photodissociation of SiH_4:

$$n(SiH_4)^0 = n(SiH_4) + 2n(Si_2H_6) + n(Si) \quad (1)$$

Material-balance during the photodissociation of Si_2H_6:

$$2n(Si_2H_6)^0 = n(SiH_4) + 2n(Si_2H_6) + n(Si) \quad (2)$$

where n is the number of moles of the considered species, $(SiH_4)^0$ and $(Si_2H_6)^0$ are related to the initial concentration of SiH_4 and Si_2H_6, respectively.

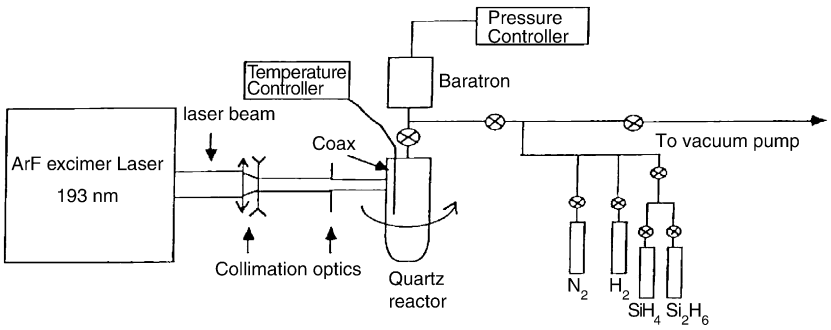

Fig. 1. Schematic diagram of the experimental set-up for the photolysis.

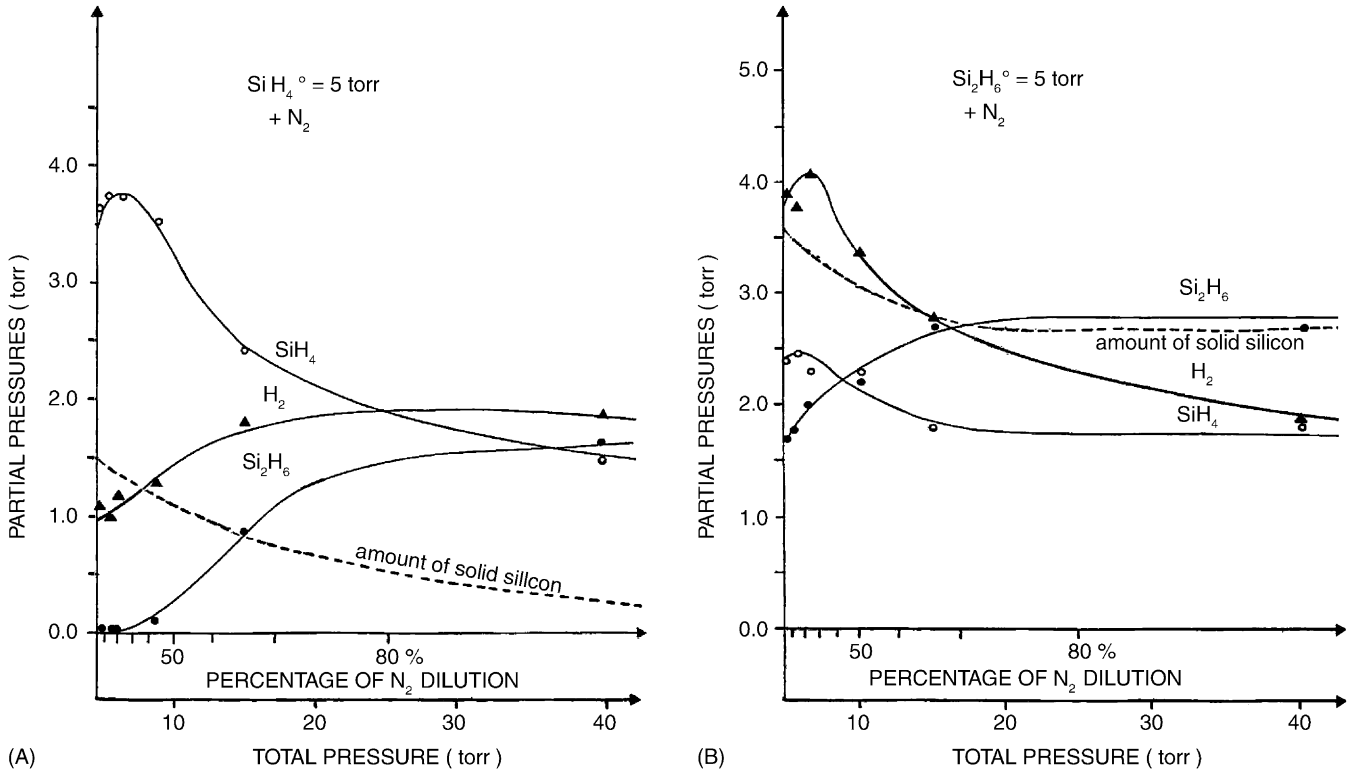

Fig. 2. Partial pressure of stable species formed during the photo-CVD, versus nitrogen pressure and total pressure: the amount of solid silicon has been deduced by mass-balance from SiH_4 and Si_2H_6 graphs (A) $(SiH_4)^0 = 5$ Torr and (B) $(Si_2H_6)^0 = 5$ Torr.

This quantity of silicon atoms is then converted to its equivalent-Torr, supposing that they exist in the gas phase: for the used cell of 71 cm^3, 1 equiv. Torr corresponds to $(3.28 \times 10^{16} \times 71 \times 28)/N \approx 1.1 \times 10^{-4}$ g of silicon, where N is the Avogadro's number, 28 the atomic mass of silicon and 3.28×10^{16} the number of gaseous atoms or molecules per cubic centimetre at 1 Torr pressure.

We report only the main reactions necessary for the understanding of the role of the dilution and their kinetic constants at room temperature.

Fig. 2A and B, relative to 5 Torr of initial silane and disilane pressure, respectively, shows the final pressures of SiH_4, Si_2H_6 and H_2 and the evolution of the amount of solid silicon (Si) formed.

In Fig. 2A, we note that the partial pressure of the reactant SiH_4 decreases drastically with increasing the total pressure and dilution, whereas those of the gaseous products H_2 and Si_2H_6 increase. This can be explained by secondary reactions which lead to the subsequent consumption of SiH_4 and the formation of Si_2H_6 via activation reactions (R_7) and (R_8) followed by the deactivation or thermalization reactions (R_9) and (R_{10}):

$$SiH_2 + SiH_4 \rightarrow Si_2H_6^*, \quad k_7 = 9.4 \times 10^{-13}\ cm^3\ molecule^{-1}\ s^{-1} \qquad (R_7)$$

$$SiH_3 + SiH_3 \rightarrow Si_2H_6^{**}, \quad k_8 = 3 \times 10^{-10}\ cm^3\ molecule^{-1}\ s^{-1} \qquad (R_8)$$

$$Si_2H_6^* + M \rightarrow Si_2H_6 + M, \quad k_9 = 1.7 \times 10^{-11}\ cm^3\ molecule^{-1}\ s^{-1} \qquad (R_9)$$

$$Si_2H_6^{**} + M \rightarrow Si_2H_6 + M, \quad \Delta H = -305\ kJ/mol,\ k_{10}\ \text{is unknown} \qquad (R_{10})$$

The excited species $Si_2H_6^*$ and $Si_2H_6^{**}$ resulting from silene (SiH_2) insertion into silane (reaction (R_7)) and silyl (SiH_3) radical recombination (reaction (R_8)) present an excess energy of 205 kJ/mol (2.1 eV) and 305 kJ/mol (3.2 eV), respectively [23,24]; they are stabilized by transfer of energy when colliding a buffer gas molecule M (reactions (R_9) and (R_{10})). The increase of H_2 gas could be interpreted by the following reaction which also contributes to the depletion of the reactant gas SiH_4:

$$H + SiH_4 \rightarrow SiH_3 + H_2, \quad k_{11} = 4.3 \times 10^{-13}\ cm^3\ molecule^{-1}\ s^{-1} \qquad (R_{11})$$

However, at 0% dilution (i.e. pure SiH_4), the Si_2H_6 produced is negligible, so in this condition, the thermalization reactions (R_9) and (R_{10}), which first led to the formation of

Si_2H_6, practically do not occur in our experimental conditions, the same goes for all the reactions which necessitate disilicon species (Si_2H_n) as reactant.

Since the evolution of the gaseous species is not continuous, it would be delayed by some reactions such as

$$H + Si_2H_6 \rightarrow SiH_3 + SiH_4,$$
$$k_{12} = 1.1 \times 10^{-12}\,cm^3\,molecule^{-1}\,s^{-1} \quad (R_{12})$$

$$SiH_2 + H_2 \rightarrow SiH_4,$$
$$k_{13} = 1 \times 10^{-13}\,cm^3\,molecule^{-1}\,s^{-1} \quad (R_{13})$$

$$SiH_3 + SiH_3 \rightarrow SiH_2 + SiH_4,$$
$$k_{14} = 1.5 \times 10^{-10}\,cm^3\,molecule^{-1}\,s^{-1} \quad (R_{14})$$

Reaction (R_{14}), despite its high rate constant, would have a small contribution as seen by the relative primary quantity of SiH_3 radicals produced during the silane photolysis (for example, the primary quantum yields are $\phi(SiH_2) = 0.83$ and $\phi(SiH_3) = 0.17$ at the wavelength of 147 nm) [23].

Moreover, the reactions (R_8) and (R_{14}) of silyl recombination should be in competition as seen the similar value of their rate constants but, in reality (R_{14}) occurs consecutively the appearance of $Si_2H_6^{**}$ by the process [13,23]:

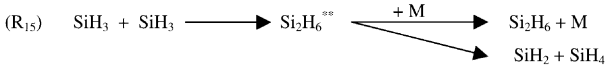

(R_{15})

So, when dilution is increasing the thermalization reaction (R_{10}) would be favoured.

In contrast to the reactant SiH_4 photodecomposition, we can see at Fig. 2B that the pressure of the reactant gas Si_2H_6 increases (i.e. its conversion decreases) and those of the gaseous products H_2 and SiH_4 decrease with increasing the dilution; in this case, at 0% dilution (i.e. undiluted disilane), the concentration of each product is more than that of the reactant Si_2H_6. This is due to its fast rate of decomposition [31]. The early production of SiH_4 is likely due to the reactions ((R_{12})–(R_{14})) as seen the large primary production of SiH_3, SiH_2 and H radicals (for example $\phi(R_6) = 0.61$ at 147 nm) [24] which will favour these radicals reactions ((R_{12})–(R_{14})) and the following reaction (R_{16}) which also leads to H_2 formation:

$$H + Si_2H_6 \rightarrow Si_2H_5 + H_2,$$
$$k_{16} = 2.1 \times 10^{-12}\,cm^3\,molecule^{-1}\,s^{-1} \quad (R_{16})$$

Therefore, at 0% dilution in absence of buffer gas, the excited disilane undergoes decomposition through the following reactions

$$Si_2H_6^* \rightarrow SiH_3SiH + H_2, \quad \Delta H = -15\,kJ/mol \quad (R_{17})$$

$$Si_2H_6^{**} \rightarrow SiH_2 + SiH_4, \quad \Delta H = -66\,kJ/mol \quad (R_{18})$$

$$Si_2H_6^{**} \rightarrow SiH_3SiH + H_2, \quad \Delta H = -115\,kJ/mol \quad (R_{19})$$

The thermalization reaction (R_9) becomes more and more important for increasing nitrogen concentration in accord with Austin et al. [18,19] report as $k_9[M] \gg k_{17}$; so, the reactions (R_{10}) and (R_{18}) are less efficient than the reaction (R_{19}) because $k_{19} \gg k_{18} + k_{10}[M]$. Nevertheless, the probability of thermalization reaction (R_{10}) increases with pressure to the detriment of reaction (R_{18}) as seen previously. Thus, reaction (R_{19}) is certainly the most likely path in the dissociation of excited disilane $Si_2H_6^{**}$.

In the two cases of silane and disilane photodecomposition, the amount of Si formed decreases with increasing the dilution and its value is the greatest at 0% dilution. For any dilution, the amount of Si formed is greater when using Si_2H_6 as the reactant.

Similarly, we compare Fig. 3A with Fig. 3B in the case of the initial reactant gas pressure of 12 Torr. We can observe in Fig. 3A that the evolution of the species is less drastic than that of graphs in Fig. 2A which is related to the initial silane pressure of 5 Torr; moreover, in these two later figures, the trends of the gaseous species vary in the opposite way. However, this is not evident for the product Si_2H_6 since total pressure is limited to 40 Torr in Fig. 2A, but in both the cases, the fraction of disilane produced at 0% dilution is negligible. In Fig. 3A, SiH_4 rises slightly and the product Si_2H_6 reaches a maximum (less than 5% of gas composition) near total pressure of 40–50 Torr corresponding to about 60–70% dilution before decreasing. We note that the fraction of products (H_2, Si_2H_6, solid Si) decrease with increasing the initial silane pressure; this is the consequence of the augmentation of SiH_4 pressure which could be explained by the relative importance of reactions such as (R_{13}) and (R_{18}) which favour the reformation of SiH_4 molecules.

In the case of disilane photolysis, when looking at Fig. 3B, all partial pressures evolve in a similar way like Fig. 2B relative to the initial disilane pressure of 5 Torr: the reactant Si_2H_6 pressure first increases and those of the product SiH_4 decreases; the same behaviour is observed in Fig. 4B in the case of Si_2H_6 initial pressure of 20 Torr while in Fig. 4A under the identical conditions of dilution for SiH_4 reactant, all curves exhibit practically a plateau and Si_2H_6 generated remains very low. In this latter case, the decrease of radicals will reduce the formation of stable species.

In all the initial reactant pressure of disilane photodecomposition not taking into account the error level of condensation technique, the early and abrupt rising before decreasing of silane as a function of dilution is likely to be due to the rapid radical recombination reaction (R_{20}) (just after their creation):

$$SiH_3 + H \rightarrow SiH_4,$$
$$k_{20} = 5 \times 10^{-10}\,cm^3\,molecule^{-1}\,s^{-1} \quad (R_{20})$$

and the early rise in the disilane concentration should be due to the reaction (R_{21}) which reforms Si_2H_6 molecules:

$$Si_2H_5 + H \rightarrow Si_2H_6, \quad \text{supposing } k_{21} \approx k_{20} \quad (R_{21})$$

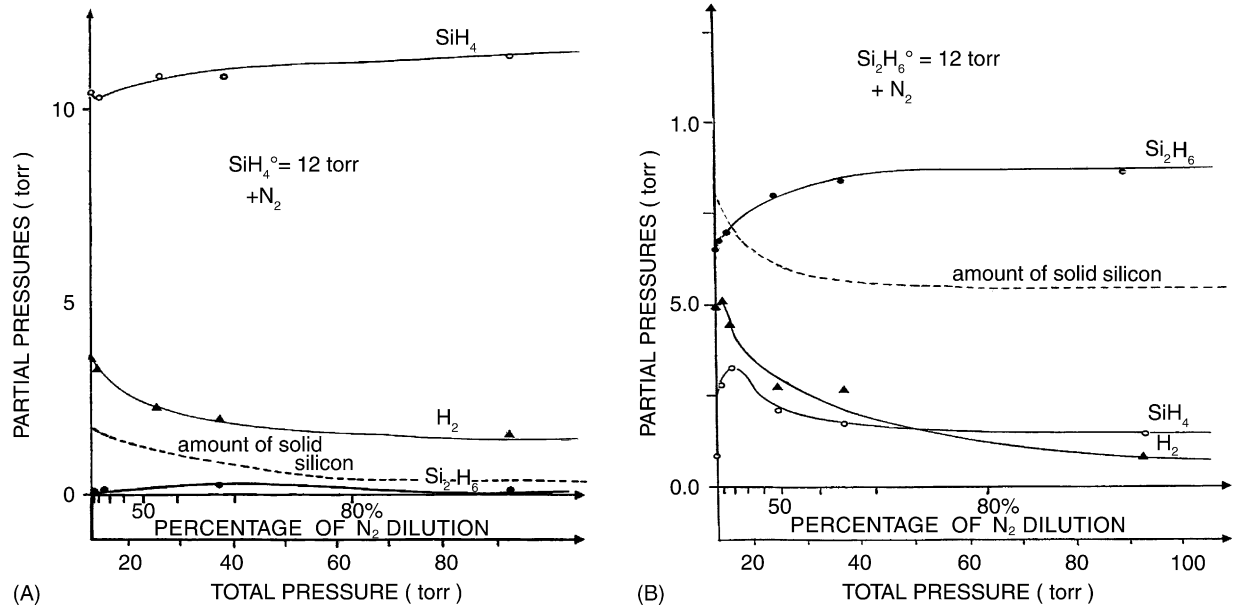

Fig. 3. Partial pressure of stable species formed during the photo-CVD, as a function of nitrogen pressure and total pressure: (A) $(SiH_4)^0 = 12$ Torr; (B) $(Si_2H_6)^0 = 12$ Torr.

In the case of Si_2H_6 photolysis (Figs. 2–4B), we note that the concentration of H_2 produced is more than that of SiH_4 produced below total pressure of 40–50 Torr, after which they reach approximately a stationary and equivalent value.

We can note that (Si_2H_n) radicals are significant only in the primary steps of Si_2H_6 photolysis; the production of Si_2H_6 molecules depends on the generation of radicals SiH_2 and SiH_3 which lead, respectively, to the formation of excited $Si_2H_6^*$ (reaction (R_7)) and $Si_2H_6^{**}$ (reaction (R_8)) which rather decompose at lower pressure (reactions (R_{17})–(R_{19})) because only the total pressure in the cell has an effect on the mean free path l of the molecules which simply can be defined by

$$l = \frac{k_B T}{(\sqrt{2} P \pi \sigma^2)} \tag{3}$$

where k_B is the Boltzmann constant, T the absolute temperature into the cell, P the total gas pressure, σ^2 the quenching cross-section. The radicals just created by the photon absorption of the reactant gas will cover a shorter distance at high

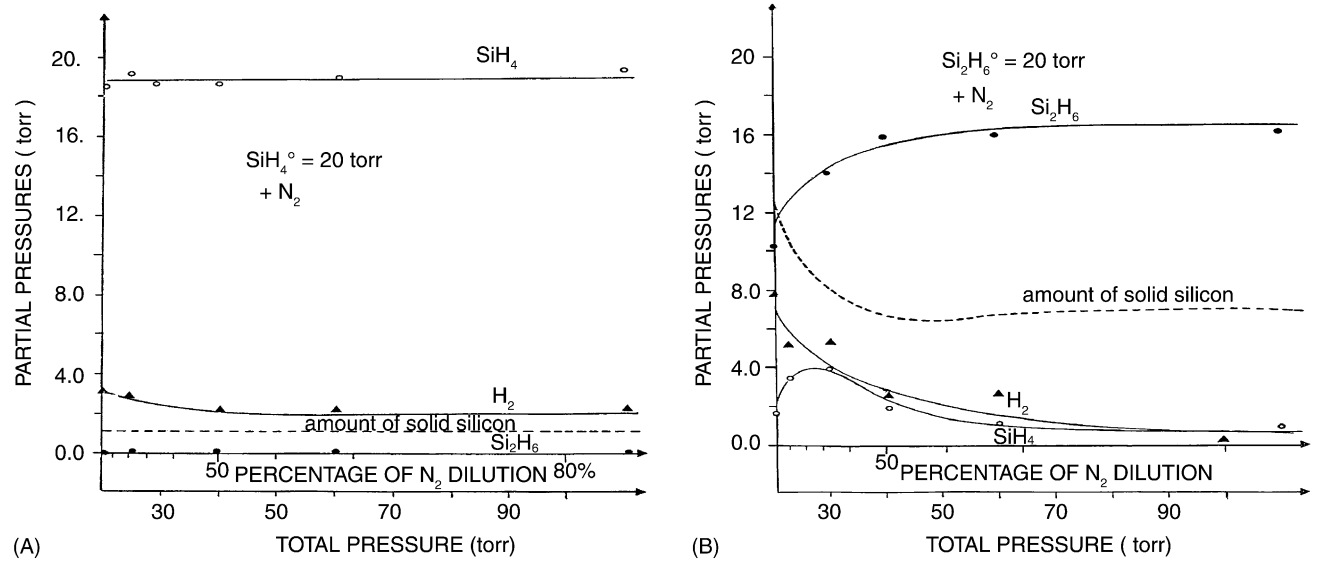

Fig. 4. Partial pressure of stable species formed during the photo-CVD, as a function of nitrogen pressure and total pressure: (A) $(SiH_4)^0 = 20$ Torr; (B) $(Si_2H_6)^0 = 20$ Torr.

total pressure because of the rising of collisions between the gaseous species; hence, their probability to recombine and form the initial molecule will become important.

In all the figures, a pressure steady-state is reached above 40–50 Torr of total pressure, independent of the extent of dilution. Herein, we can conclude that thermalization is the major mechanism to form or reform disilane during the SiH_4 photolysis and radical recombination is the major mechanism to form or reform silane during the Si_2H_6 photolysis.

In all the cases, the amount of solid silicon (Si) exhibits approximately the same evolution and the undiluted reactant gas leads to greater silicon formation.

We observe two total pressure regions: below 40–50 Torr, the variations of the curves are important, but above these values, the concentration of the reactant and all the products has the tendency to stay constant. However, the constant decrease in H_2 concentration, even at high total pressure, particularly in the Si_2H_6 photolysis, is probably due to the continuous adsorption of hydrogen atoms followed by their incorporation into solid silicon since, for example, the equivalent-pressure of Si formed at 20 Torr of Si_2H_6 initial reactant pressure is 8 Torr against 1 Torr in that of SiH_4.

As a consequence, at high total pressure, the dilution has no more effects on the kinetics: the molecular density is high enough to induce a saturation on the phenomena related to the pressure of an inert gas. The silicon which is in the solid phase follows an equivalent behaviour and tends to saturate at high pressure. So, a true pressure equilibrium-state is only reached in the high total pressure limits, above 50 Torr.

3.2. Influence of nitrogen dilution on deposition yield

In the photo-CVD techniques, the control of the thickness in other words the amount of silicon deposited is the final aim. From the material-balance relations (1) and (2), we deduce the expression of deposition yield η_d which best express the efficiency of the gaseous reactant conversion into solid phase silicon. First, during the photodissociation of SiH_4

$$\eta_d = \frac{n(Si)}{n(SiH_4)^0} = 1 - \frac{[n(SiH_4) + 2n(Si_2H_6)]}{n(SiH_4)^0} \quad (4)$$

secondly, during the photodissociation of Si_2H_6

$$\eta_d = \frac{n(Si)}{2n(Si_2H_6)^0} = 1 - \frac{[n(SiH_4) + 2n(Si_2H_6)]}{2n(Si_2H_6)^0} \quad (5)$$

The diffusion of free silicon hydride radicals towards the wall leads to a surface reaction followed by film-deposition in a hydrogenated amorphous (or powder) silicon SiH_x form where x is a stoichiometric coefficient [19,23–25,29]:

$$SiH_3 + \text{wall} \rightarrow SiH_x(s) + \tfrac{1}{2}(3-x)H_2 \quad (R_{22})$$

$$SiH_2 + \text{wall} \rightarrow SiH_x(s) + \tfrac{1}{2}(2-x)H_2 \quad (R_{23})$$

$$SiH_3SiH_2 + \text{wall} \rightarrow Si_2H_x(s) + \tfrac{1}{2}(5-x)H_2 \quad (R_{24})$$

$$SiH_3SiH + \text{wall} \rightarrow Si_2H_x(s) + \tfrac{1}{2}(4-x)H_2 \quad (R_{25})$$

knowing that the reaction (R_{24}) and (R_{25}) could be more significant only during the Si_2H_6 photolysis.

Fig. 5A and B shows the dependence of the deposition yield of silicon from silane and disilane on both nitrogen dilution and the initial reactant pressure.

These curves are in accordance with the previous explanations: the deposition yield increases with decreasing silane or disilane initial pressure but in all the cases it remains practically constant above 50% dilution. In all cases the deposition yield of silicon in Si_2H_6 photolysis is greater than that of SiH_4, remembering moreover that in this latter experiment, 1200 laser pulses are used in the Si_2H_6 photolysis against 1800 in that of SiH_4.

However, regarding the amount of Si formed when using the same reactant gas, we have verified, for example, in pure Si_2H_6 photolysis that a yield of 47% at 2 Torr corresponds to only 0.9 equiv. Torr, while 6% at 80 Torr correspond to a value of 4.8 equiv. Torr.

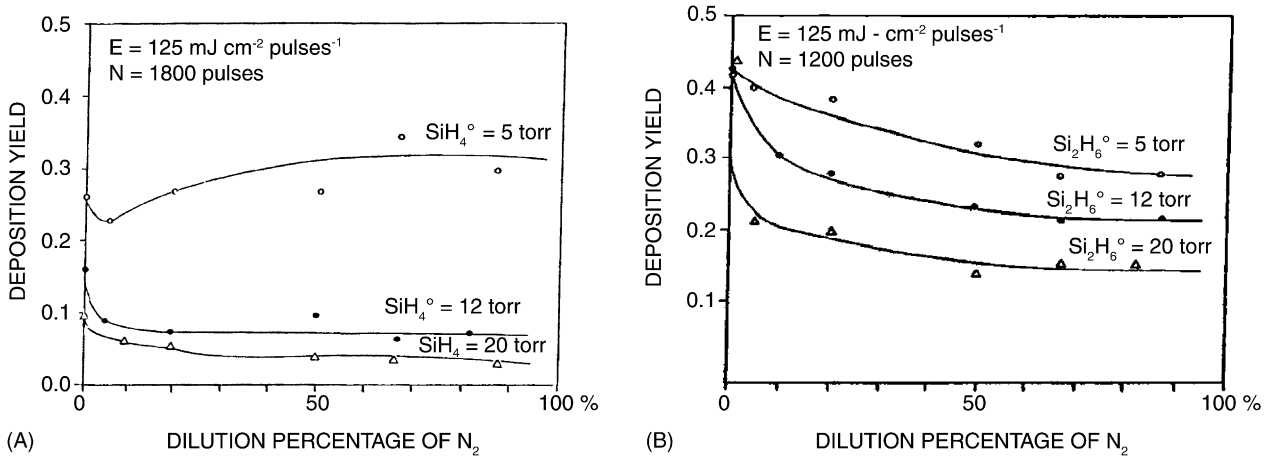

Fig. 5. Deposition yield of silicon as a function of N_2 dilution percentage, at different initial reactant pressures for: (A) SiH_4; (B) Si_2H_6.

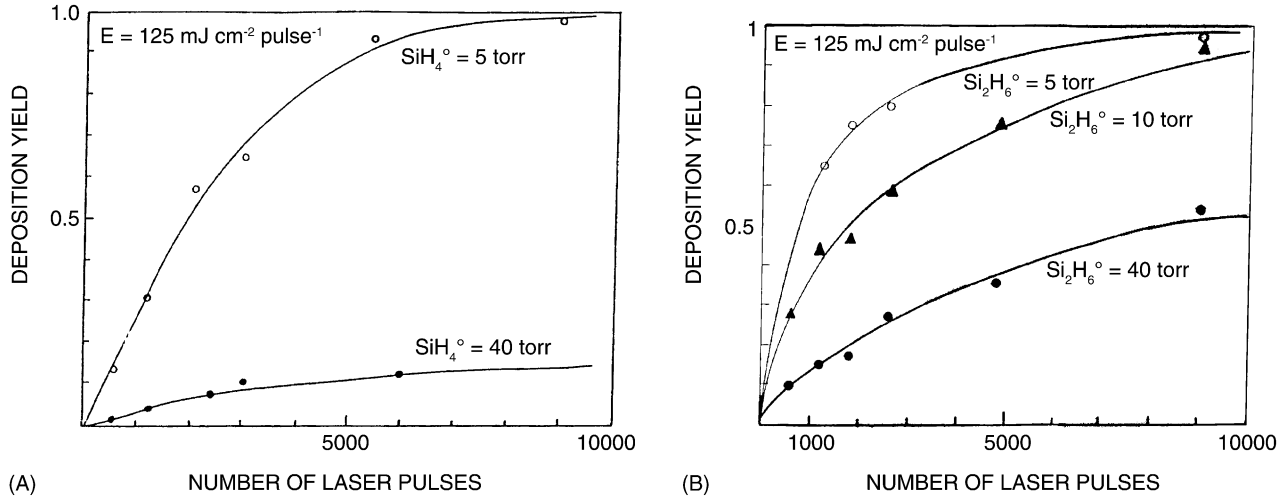

Fig. 6. Deposition yield of silicon versus irradiation time (in number of laser pulses) of reactant gas, at different initial pressure for pure: (A) SiH_4; (B) Si_2H_6.

We show in Fig. 6A and B the effect of both the initial pressure of undiluted reactant gas (pure SiH_4 or pure Si_2H_6) and the irradiation time (in number of laser pulses) on the deposition yield. Looking at the two figures, the deposition yield increases with increasing the irradiation time but for lower initial reactant pressure (5 Torr and below) this value quickly reaches a time steady-state from about 5000 pulses (∼8 min), though this is not so pronounced at higher pressures which need a longer time, particularly in the Si_2H_6 photolysis.

This behaviour observed in the condition of pure reactant gas can be explained by an equilibrium gas phase–solid phase, if we assume that no decrease in transparency of the tube wall appear under our experimental conditions; the true irradiation time-equilibrium-state is only reached in the low initial pressure limits contrary to that observed during incoherent lamps photo-CVD [15,21,23–25,28].

Finally, the deposition yield, in other words, the deposition rate is larger in the Si_2H_6 photodissociation than that of SiH_4 for all initial reactants pressure and all laser pulses; it is known that Si_2H_6 is less stable than SiH_4, so it decomposes naturally more quickly than SiH_4 [27,31].

3.3. Simulation of the reaction model

For a better understanding of the experimental results, the kinetic scheme model describing the main photochemical processes has been computed in the case of silane for which all the rate constants of the elementary reactions are known. Under the conditions of pure reactant gas at relatively lower pressure (5 and 12 Torr), the radical recombination reactions are reduced and no effect of thermalization reactions exist.

Complying with the above explanations, the kinetic mechanism has been simplified and similar to that we have previously proposed in the mercury-sensitized photo-CVD of SiH_4 [21,25].

The system of non-linear differential equations, deduced from the following reactions and assuming that hydrogenation rate of deposited silicon is negligible ($x = 0$), has been resolved as a function of irradiation time in number of laser pulses:

$$SiH_4 + 2h\nu \xrightarrow{193\,nm} SiH_3 + H, \quad {}^*\phi = 0.17 \qquad (R_1)$$

$$SiH_4 + 2h\nu \xrightarrow{193\,nm} SiH_2 + 2H, \quad \phi = 0.83 \qquad (R_2)$$

$$H + SiH_4 \rightarrow SiH_3 + H_2,$$
$$k_{11} = 4.3 \times 10^{-13}\,cm^3\,molecule^{-1}\,s^{-1} \qquad (R_{11})$$

$$SiH_3 + SiH_3 \rightarrow SiH_2 + SiH_4,$$
$$k_{14} = 1.5 \times 10^{-10}\,cm^3\,molecule^{-1}\,s^{-1} \qquad (R_{14})$$

$$SiH_2 + SiH_4 \rightarrow Si_2H_6^*,$$
$$k_7 = 9.4 \times 10^{-13}\,cm^3\,molecule^{-1}\,s^{-1} \qquad (R_7)$$

$$H + Si_2H_6 \rightarrow SiH_3 + SiH_4,$$
$$k_{12} = 1.1 \times 10^{-12}\,cm^3\,molecule^{-1}\,s^{-1} \qquad (R_{12})$$

$$SiH_2 + H_2 \rightarrow SiH_4,$$
$$k_{13} = 1 \times 10^{-13}\,cm^3\,molecule^{-1}\,s^{-1} \qquad (R_{13})$$

$$SiH_3 + \text{wall} \rightarrow Si(s) + \tfrac{3}{2}H_2, \quad k_{22} = 1.5 \times 10^3\,s^{-1} \qquad (R_{22})$$

$$SiH_2 + \text{wall} \rightarrow Si(s) + H_2, \quad k_{22} = 7.5 \times 10^3\,s^{-1} \qquad (R_{23})$$

$*$ refers to arbitrary ϕ values corresponding to 147 nm wavelength [23,24].

Fig. 7A and B, relative to the initial silane pressures of 5 and 12 Torr, respectively, shows the evolution of the computed partial pressures of the stable gaseous species

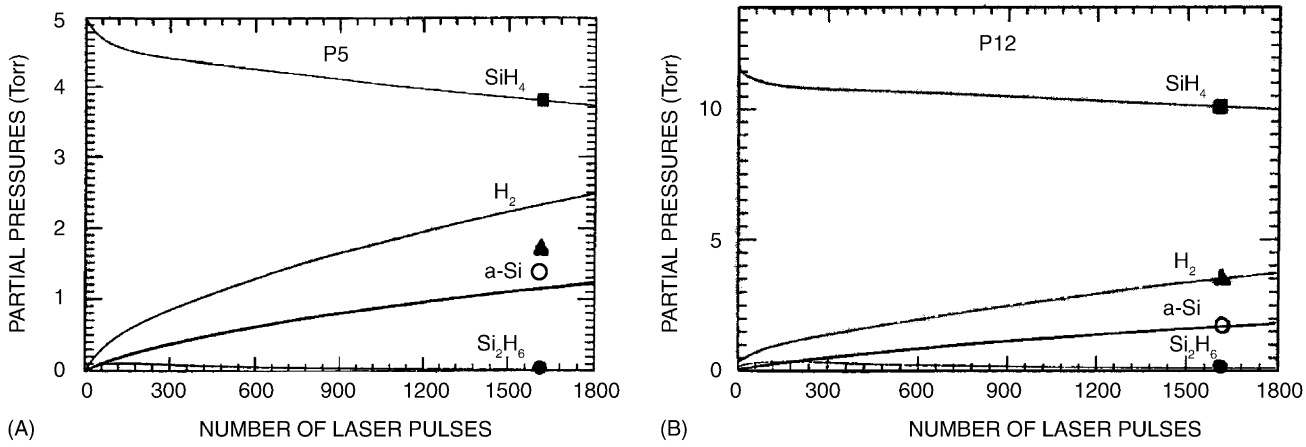

Fig. 7. Computed gas phase composition and amount of silicon deposited as a function of the irradiation time in the case of pure SiH_4: (A) $(SiH_4)^0 = 5$ Torr; (B) $(SiH_4)^0 = 12$ Torr. The experimental values at 1600 laser pulses are also shown: (■) SiH_4, (●) Si_2H_6, (▲) H_2, (○) a-Si.

(SiH_4, Si_2H_6, H_2) and the equivalent-Torr of silicon deposited (a-Si); moreover also shown on the curves are the experimental values of these various species obtained at 1600 laser pulses. Taking into account the error level of condensation technique, up to 10–15% in lower pressure region below 5 Torr, we can assert that these calculated curves are in good accordance with the experimental observations.

4. Conclusion

The experiments show that the gas composition and the deposition yield of the reactant depend on nitrogen dilution during silane and disilane laser photo-CVD at 193 nm.

During the silane photodissociation at the initial reactant pressure below 5 Torr, the concentration of silane decreases (i.e. its conversion increases) with increasing dilution, and at higher initial reactant pressure the conversion of silane and the concentration of the other stable species tend to stay constant with increasing dilution. In contrast, at any initial reactant pressure, the conversion of disilane during its photodecomposition decreases with increasing dilution tending to reach a concentration stationary-state at large dilution.

We have observed two total pressure regions, independent of the dilution: below 40–50 Torr, the variations of stable species concentrations are very important but above these values they have the tendency to stay constant.

In the two cases of silane and disilane photodissociation, the amount of solid silicon formed is greater when using undiluted reactant gas. In addition, in all the cases it is greater with disilane as the reactant rather than of silane.

The deposition yield of silicon increases when decreasing the initial reactant gas pressure and a pressure stationary-state was observed from about 50% dilution and an irradiation time stationary-state from about 5000 pulses.

We note that radical recombination is the major mechanism to form silane and thermalization is the major mechanism to form disilane.

The chemical kinetic reactions, studied in a sealed reactor are also available under gas flow conditions and dilution will induce the same overall behaviour because above 50% dilution, the deposition yield will not be affected by small variations in total pressure. This makes easier the use of buffer gases for different technical reasons (e.g. window blowing to prevent opacification) during the photo-CVD deposition technique.

A reaction model applied to limited conditions is proposed for which computed results are shown to be in agreement with the experimental measurements.

Acknowledgements

This work was performed at the “Centre de Recherches Nucléaires—Laboratoire PHASE” of Strasbourg, France. The authors would like to sincerely express their gratitude to Dr. C. Fuchs and Dr. E. Fogarassy of PHASE Laboratory for their helpful suggestions and encouragement.

References

[1] P. Boher, J.L. Stehle, E. Fogarassy, Appl. Surf. Sci. 138–139 (1999) 199.
[2] C. Fuchs, R. Henck, E. Fogarassy, J. Hommes, F. Le Normand, J. Phys. IV 9 (1999) 5.
[3] B. Aka, Phys. Chem. News 1 (2001) 47–55.
[4] J. Pola, M. Urbanova, Z. Bastl, J. Subrt, M. Sakuragi, A. Ouchi, H. Morita, Polymer (Guildford) 42 (4) (2001) 1311.
[5] W. Roth, K.W. Hoffmann, W. Kurz, J. Polym. Sci. A 32 (10) (1994) 1893.
[6] N. Banerji, J. Serra, C. Serra, S. Chiussi, F. Lusquinos, X. Redondas, B. Leon, A.M. Perez, Surf. Coat. Technol. 100–101 (1/3) (1998) 393.
[7] F. Ishihara, H. Uji, T. Kamimura, S. Mastumoto, H. Higuchi, S. Chichibu, Jpn. J. Appl. Phys. 34 (5A) (1995) 2229.
[8] N. Mutsukura, Y. Katoh, Y. Machi, J. Appl. Phys. 60 (9) (1986) 3364.
[9] T. Kamimura, M. Hirose, Jpn. J. Appl. Phys. 25 (12) (1986) 1778.

[10] P. Gonzalez, J. Pou, D. Fernandez, E. Garcia, J. Serra, B. Leon, A.M. Perez, Thin Solid Films 230 (1) (1993) 35.
[11] S. Tamir, J. Zahavo, Y. Komem, M. Eizenberg, J. Mater. Sci. 31 (4) (1996) 1013.
[12] N. Mutsukura, Y. Katoh, Y. Machi, J. Appl. Phys. 60 (9) (1986) 3364.
[13] M. Koshi, A. Miyoshi, H. Matsui, Chem. Phys. Lett. 184 (5–6) (1991) 442.
[14] Y. Toyoshima, K. Kumata, U. Itoh, A. Matsuda, Appl. Phys. Lett. 51 (23) (1987) 1925.
[15] J. Blazejowsk, F.W. Lampe, J. Photochem. 20 (1982) 9.
[16] P.A. Longeway, F.W. Lampe, J. Am. Chem. Soc. 103 (1981) 6813.
[17] R. Robertson, A. Gallagher, J. Appl. Phys. 59 (10) (1986) 3402.
[18] E.R. Austin, F.W. Lampe, J. Phys. Chem. 80 (26) (1976) 2811.
[19] E.R. Austin, F.W. Lampe, J. Phys. Chem. 81 (12) (1977) 1134.
[20] C. Fuchs, E. Boch, E. Fogarassy, B. Aka, P. Siffert, Materials Research Society (MRS) Proceedings, Vol. 101, Boston, USA, 1988, pp. 361–365.
[21] B. Aka, Thèse de l'Université Louis Pasteur-Strasbourg 1, CRN/CPR 89–02, No. d'ordre 607, Avril 1989.
[22] E. Boch, Thèse de l'Université Louis Pasteur-Strasbourg 1, CRN/CPR 90–05, No. d'ordre 905, Octobre 1990.
[23] G.C.A. Perkins, E.R. Austin, F.W. Lampe, J. Am. Chem. Soc. 101 (5) (1979) 1109.
[24] G.C.A. Perkins, E.R. Austin, F.W. Lampe, J. Am. Chem. Soc. 102 (11) (1980) 3764.
[25] B. Aka, C. Fuchs, E. Fogarassy, P. Siffert, European Materials Research Society (E-MRS) Proceedings, Vol. XV, Strasbourg, June 1987, Les Éditions de Physique, Paris, pp. 147–152.
[26] R. Becera, M. Ponz, M. Castillejo, M. Oujja, J. Ruiz, M. Martin, J. Photochem. Photobiol. A 101 (1) (1996) 1.
[27] T.L. Pollock, H.S. Sandhu, A. Jodhan, O.P. Strausz, J. Am. Chem. Soc. 95 (4) (1973) 1017.
[28] B. Aka, A. Trokourey, J. Soc. Ouest Afr. Chim. 9 (2000) 27.
[29] J. Perrin, T. Broekhuizen, Appl. Phys. Lett. 50 (8) (1987) 433.
[30] D. Metzger, K. Hesch, P. Hess, Appl. Phys. A 45 (1988) 345.
[31] M. Bowrey, J.H. Purnell, Proc. Roy. Soc. Lond. A 321 (1971) 341–359.
[32] A. Watanabe, K. Osato, S. Ninomiya, M. Mukaida, T. Tsunoda, Y. Imai, Thin Solid Films 274 (1–2) (1996) 70.